PROTEINS: Structure, Function, and Bioinformatics 65:87–102 (2006)

Electrostatic Contribution to the Binding Stability of Protein–Protein Complexes

Feng Dong[1] **and Huan-Xiang Zhou**[2*]
[1]*Department of Physics, Drexel University, Philadelphia, Pennsylvania*
[2]*Department of Physics and Institute of Molecular Biophysics and School of Computational Science, Florida State University, Tallahassee, Florida*

ABSTRACT **To investigate roles of electrostatic interactions in protein binding stability, electrostatic calculations were carried out on a set of 64 mutations over six protein–protein complexes. These mutations alter polar interactions across the interface and were selected for putative dominance of electrostatic contributions to the binding stability. Three protocols of implementing the Poisson-Boltzmann model were tested. In vdW4 the dielectric boundary between the protein low dielectric and the solvent high dielectric is defined as the protein van der Waals surface and the protein dielectric constant is set to 4. In SE4 and SE20, the dielectric boundary is defined as the surface of the protein interior inaccessible to a 1.4-Å solvent probe, and the protein dielectric constant is set to 4 and 20, respectively. In line with earlier studies on the barnase–barstar complex, the vdW4 results on the large set of mutations showed the closest agreement with experimental data. The agreement between vdW4 and experiment supports the contention of dominant electrostatic contributions for the mutations, but their differences also suggest van der Waals and hydrophobic contributions. The results presented here will serve as a guide for future refinement in electrostatic calculation and inclusion of nonelectrostatic effects. Proteins 2006;65:87–102.** © 2006 Wiley-Liss, Inc.

Key words: protein complex; binding stability; electrostatic interactions; ion pairs; Poisson-Boltzmann equation

INTRODUCTION

Most proteins function by interacting with other proteins, DNA, and RNA. The stability of the resulting specific protein complexes is thus of fundamental importance. Similar to the folding stability of proteins, the binding stability must arise from specific interactions formed upon complexation. However, some of the most basic questions on binding stability remain unsettled. The association constant (K_a) varies from 10^{15} to $<10^3$ M^{-1}. It is not clear how the variation of K_a by orders of magnitude can be explained.[1] While the contribution of hydrophobic interactions to binding (and folding) stability is universally accepted, the role of electrostatic interactions is still controversial.[2] We have carried out systematic computational studies on the contributions of electrostatic interactions to protein folding stability[3–6] and have begun such studies on protein binding stability.[2] The approach is to directly assess the computed effects of a large number of charge and polar mutations against experimental results on stability. The assessment serves both to discriminate calculation protocols and to generate insight on electrostatic contributions. In this paper we extend the study of electrostatic contributions to a set of 64 mutations on six protein–protein complexes.

The six protein complexes have association constants ranging from $\sim 10^{14}$ to $<10^6$ M^{-1} [Table I; Fig. 1(a)] and in each case, electrostatic contributions have been suggested.[7–15]

- Interleukin-4 (IL4), a four-helix bundle cytokine, forms a tight complex with the extracellular domain of the α chain (IL4BP) of the receptor.[16] An ion pair between IL4_R88 and IL4BP_D72 makes a major contribution to the binding stability [Fig. 1(b)].[7,16] Ionic strength is found to exert a strong effect on the association rate but a weak effect on the dissociation rate,[8] demonstrating that long-range electrostatic interactions in this complex enhance the rate of complex formation and stabilize the bound state.[17]
- The 12-kD FK506-binding protein (FKBP), upon binding FK506, acts as a high-affinity inhibitor of calcineurin (CN) [Fig. 1(c)].[18] Several charged residues (e.g., Arg42) of FKBP have been implicated in its interaction with CN through mutational studies.[9,10]
- Rap1A is a Ras-like GTPase that binds with, among other targets, the Ras-binding domain of the Sre/Thr-specific protein kinase c-Raf1 [Fig. 1(d)].[19] The interface

Feng Dong's present address is Department of Biochemistry and Molecular Biophysics, Washington University in St. Louis, St. Louis, MO 63110.

*Correspondence to: Huan-Xiang Zhou, Department of Physics and Institute of Molecular Biophysics and School of Computational Science, Florida State University, Tallahassee, FL 32306. E-mail: zhou@sb.fsu.edu

Received 28 November 2005; Revised 10 February 2006; Accepted 29 March 2006

Published online 19 July 2006 in Wiley InterScience (www.interscience.wiley.com). DOI: 10.1002/prot.21070

TABLE I. Overall Properties of Six Protein Complexes

			Protein A[c]		Protein B[c]	
Complex	K_a[a] (10^9 M^{-1})	PDB[b]	Number of residues[d]	Net charge[e]	Number of residues[d]	Net charge[e]
IL4:IL4BP	6.7	liarA:B	129(1–129)	+7 (9/12|4/10)	188 (1–107, 112–163, 169–197)	−5 (7/6|9/9)
FKBP:CN	0.13–0.18	1tcoC:(A; B)[f]	107(1–107)	+1 (6/8|6/7)	352;169 (21–372;1–169)	−8;−11 (17/18|21/22; 6/15|19/13)
Rap1 A:Raf1	8.3×10^{-4}	1clyA:B	167(1–167)	−6(9/10|12/13)	77 (55–131)	+4 (6/6|4/4)
CD2:CD58	3.3×10^{-3}	1qa9A:B	101(4–105)	−1 (2/18|13/8)	95 (1–95)	−3 (2/9|5/9)
Im9:E9	$(4.2 - 6.2) \times 10^4$	1emvA:B	86(1–86)	−9 (1/6|6/10)	134 (1–134)	+7 (8/20|7/14)
AChE:Fas	2×10^2	1mahA:F	543(1–543)	−9(37/8|27/27)	61 (1–61)	+4 (5/4|3/2)

[a]Association constants were from Zhang et al.;[7] Yang et al.[9] and Futer et al.;[10] Nassar et al.;[11] Kim et al.;[12] Wallis et al.[13,14] at ionic strength of ~225 mM; and Radic et al.[15] at ionic strength of 100 mM.
[b]X-ray structures of the complexes were determined by Hage et al.;[16] Griffith et al.;[18] Nassar et al.;[19] Wang et al.;[20] Kuhlmann et al;[21] and Bourne et al.[22] Chains making up a single complex are indicated and separated by a colon.
[c]Protein A and protein B correspond to the protein names before and after, respectively, the colon in the column under "complex."
[d]Amino acids included are given in parentheses.
[e]The total numbers of Arg, Lys, Asp, and Glu are given in the parenthesis in the form of (Arg/Lys|Asp/Glu).
[f]Calcineurin (CN) has two chains (A and B) but was treated as a single protein in the electrostatic calculations. A semicolon is used to separate information for the two chains. Its binding partner FKBP has FK506 bound.

of this complex is characterized by complementary charge interactions.[11,19]

- The interaction of CD2 and CD58 mediates cell adhesion. The X-ray structure of the adhesion domains of these two proteins reveals an interface with poor shape complementarity, perhaps partly explaining the low association constant,[12] and a high concentration of ten salt bridges and five hydrogen bonds [Fig. 1(e)].[20]
- Colicin E9 is a bacterial toxin which kills *Escherichia coli* cells through the action of an endonuclease domain. The host cell co-expresses an inhibitor, immunity protein 9 (Im9), for self-protection. E9 and Im9 forms a tight complex [Fig. 1(f)][21] with K_a approaching 10^{14} M^{-1}.[13,14] This complex also shows the telltale sign of electrostatic rate enhancement, with ionic strength having a significant effect on association rate and modest effect on dissociation rate.[14]
- Fasciculin 2 (Fas) is a polypeptide toxin that binds to acetylcholinesterase (AChE) [Fig. 1(g)],[22] an enzyme essential for the breakdown and recycling of the neural transmitter acetylcholine. Charged residues on AChE have been found to be important for the binding affinity.[15] Again, ionic strength has disparate effects on association and dissociation rates.

Our computation is based on the Poisson-Boltzmann model, which distinguishes itself among alternative approaches by its relatively low calculation cost and sound physical basis.[23–25] Many methodological advances on the application of the Poisson-Boltzmann model have been made.[26–29] However, even with this model, quantitative prediction of the electrostatic effect of point mutations on folding and binding stability faces a number of challenges. The first challenge is to properly model the structural change brought by the mutation. For cancellation of numerical errors, the protein structure should be held fixed to the largest extent possible. Typically, only the mutated residue is given a modeled conformation. It is not clear how many of the neighboring residues should be included in structural relaxation.

The second challenge arises from the nature of interactions of protein charges with the solvent, that is, water. There are two distinct (but related) solvation effects (Fig. 2). Individually each charge has strong favorable charge–dipole interactions with water. At the same time the interactions between protein charges are also screened by water. For a pair of opposite charges at a fixed distance in a given protein conformation, bringing the charges closer to the protein surface elicits two opposing effects. The stronger interactions between the charges with water lower the free energy of the protein, but the stronger screening of the charge–charge interaction by water raises the free energy of the protein. Whether the movement of the two charges produces a net favorable result depends on the balance of the two effects. Similarly, when two opposite charges are brought together by binding or folding, there are two opposite effects: the desolvation of the charges disfavors the bound state, but the newly generated interactions between the charges favor the bound state. Again, whether a net favorable result is obtained from the charges depends on the balance of two opposing effects. Moreover, this balance is very sensitive to calculation protocols, in particular, how the boundary between the protein low dielectric and the solvent high dielectric is defined. A boundary that exposes protein charges more to the solvent will yield a lower desolvation cost as well as weaker interactions between the protein charges. Ultimately, the specification of the dielectric boundary has to be settled by direct comparison with experimental data.

Experimentally measured effects of point mutations on binding stability contain both electrostatic and nonelectrostatic contributions. If it is known that for certain mutations electrostatic contributions are predominant, then direct comparison with electrostatic calculations is justi-

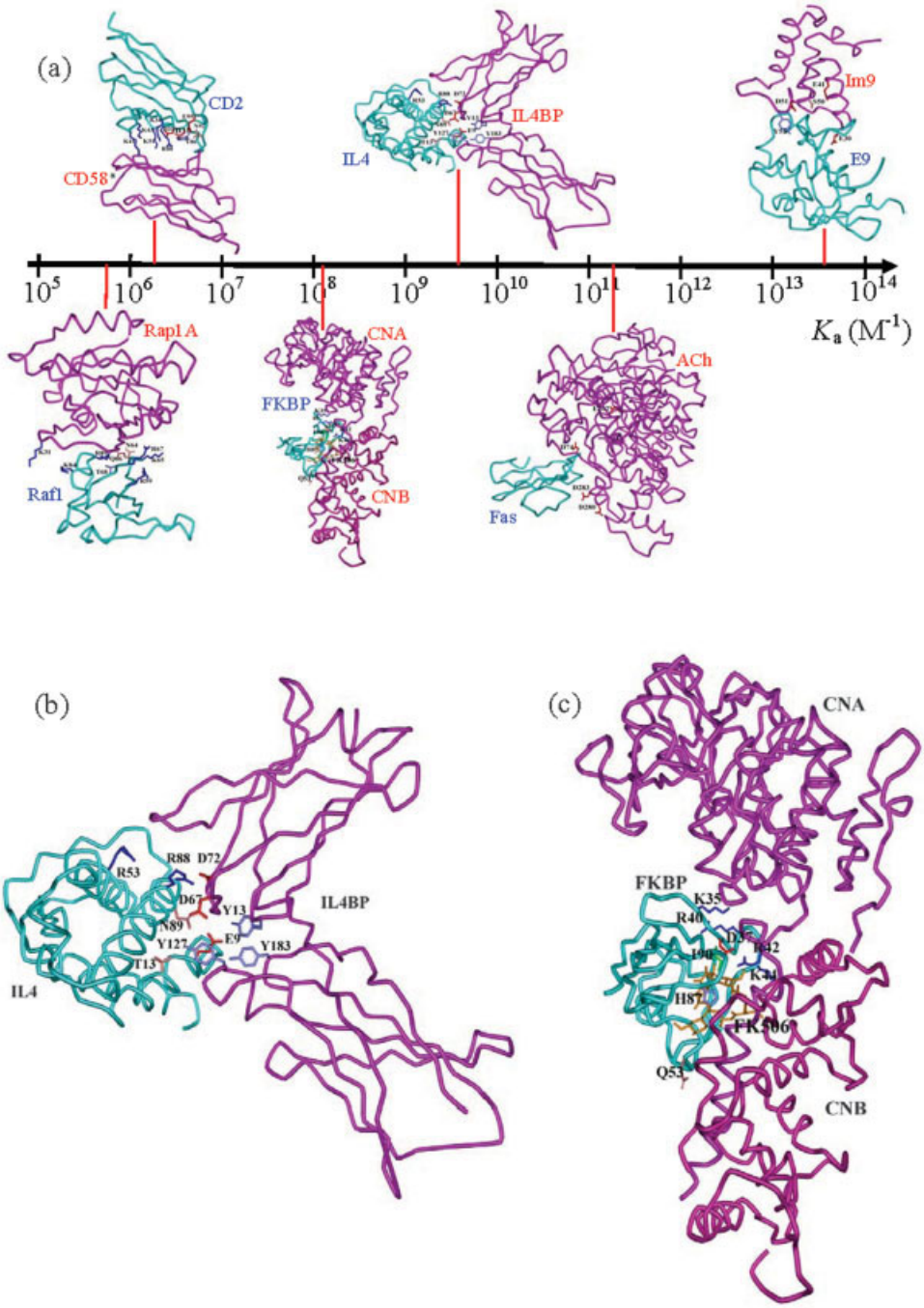

Fig. 1. Affinity and structures of six protein complexes. **a:** The six complexes span eight orders of magnitude in association constant. The structures of the complexes are enlarged in (**b**–**g**) for IL4:IL4BP, FKBP:CN, Rap1A:Raf1, CD2:CD58, Im9:E9, and AChE:Fas. Chains with positive net charges are shown in cyan; those with negative net charges are in purple. In the FKBP:CN complex, the two subunits (A and B) of CN are shown in two different shades of purple. In the CD2:CD58 complex, both chains have negative net charges; CD2 with a smaller magnitude in net charge is shown in cyan. Residues on which mutations were studied here are shown as sticks, with blue for Arg and Lys, red for Asp and Glu, light blue for Tyr and His, pink for Ser, Thr, Asn, and Gln, and green for Ile. [Color figure (parts d–h) can be viewed in the online issue, which is available at www.interscience.wiley.com.]

fied. The problem is that there is no way of knowing whether that is the case, hence the third challenge. By applying a range of calculation protocols on a large set of point mutations, we hope to get a more robust overview of electrostatic contributions to binding stability. This overview will enable us to determine when electrostatic contributions are expected to be large, hence potentially dominating, and when they are expected to be small.

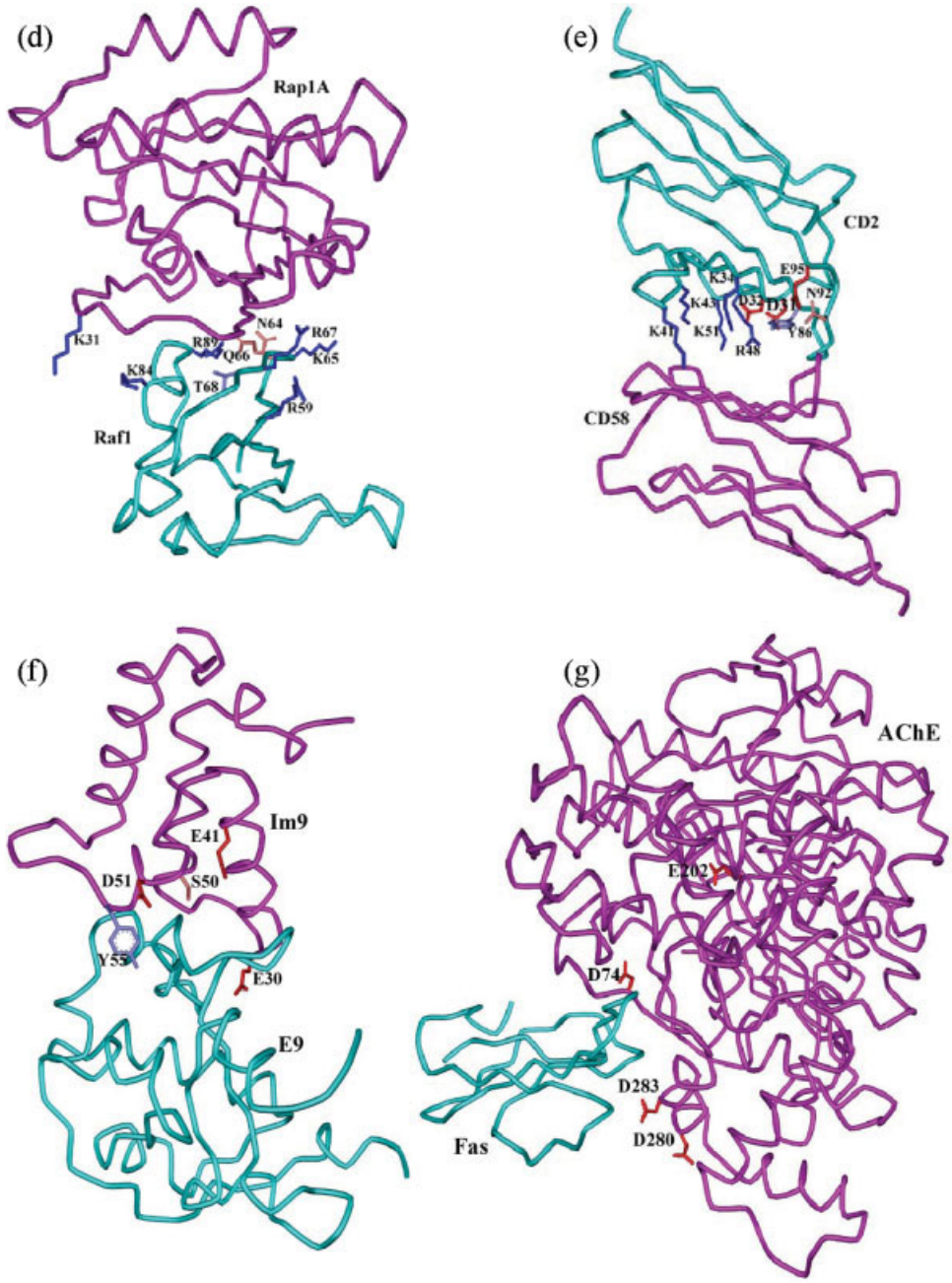

Figure 1. (Continued.)

THEORETICAL METHODS

Electrostatic Contribution to Binding Stability by Point Mutation

Suppose that protein A and protein B form a complex C with association constant K_a. Now a point mutation on protein A changes the association constant to K_a'. This change can be traced to the different effects of the mutation on the free energies of the mutation on protein A and the complex. If the free-energy changes are δG_A and δG_C, respectively, then we have

$$\delta\Delta G \equiv -k_B T \ln(K_a'/K_a) = \delta G_C - \delta G_A \quad (1)$$

where k_B is the Boltzmann constant and T is the absolute temperature. We will use "δ" to denote the change due to mutations (or ionic strength, see below) and "Δ" to denote the change due to complex formation.

In general, δG_A and δG_C will contain both electrostatic and nonelectrostatic effects. If the electrostatic effects, denoted with a subscript "el," are dominating, or alternatively, the nonelectrostatic effects in δG_A and δG_C largely cancel, then

$$\delta\Delta G \approx \delta\Delta G_{el} \equiv \delta G_{C;el} - \delta G_{A;el} \quad (2)$$

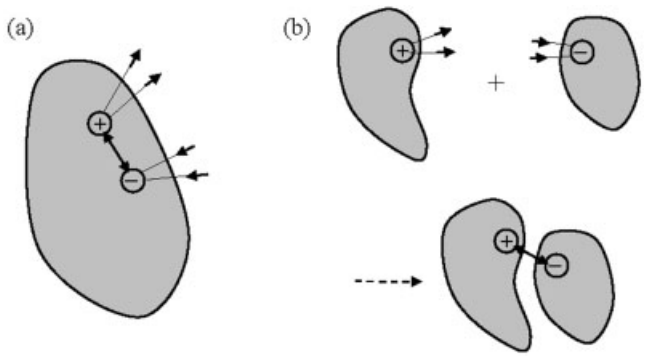

Fig. 2. Illustration of solvent effects on the electrostatic energy of a protein or protein complex. **a:** Each charge ("+" or "−") of the protein has a favorable interaction with solvent dipoles (small arrows). At the same time the solvent also screens the interaction between the charges. If the two charges were brought closer to the protein surface, the interaction of each charge with the solvent would become stronger, but the interaction between the two charges would become weaker because of increased screening by the solvent. **b:** Before two proteins form a complex, a charge on either protein has strong interaction with the solvent. After complex formation, the interaction with the solvent becomes less favorable because the charge is less accessible to the solvent, leading to desolvation cost. However, opposite charges on the two proteins, brought closer by the complex formation, will have favorable interactions and compensate for the desolvation cost.

The gist of the present study is the direct comparison of calculated $\delta\Delta G_{el}$ against experimental $\delta\Delta G$ in cases where electrostatic contributions are putatively dominating.

The overall contribution of electrostatic interactions to the binding stability is

$$\Delta G_{el} = G_{C;el} - G_{A;el} - G_{B;el} \quad (3)$$

where $G_{P;el}$ is the electrostatic free energy of protein (complex) P.

Decomposition of Electrostatic Contribution

Further insight to electrostatic contribution can be gained by decomposition:

$$G_{el} = G_{res} + G_{prot} + G_{int} \quad (4)$$

where G_{res} is the electrostatic free energy if only the residue undergoing mutation is charged, G_{prot} is the counterpart with the rest of the protein charged but the residue is completely discharged, and G_{int} results from interactions between the two parts of the protein (Fig. 3). This decomposition applies to both protein A (where the mutating residue is located) and the complex C. For protein A, the interaction is between the residue and the rest of the protein; the energy is denoted as $G_{A;int1}$. For the complex, the interaction is with the rest of protein A and with the whole protein B; the two contributions are denoted as $G_{C;int1}$ and G_{int2}. For protein B before complex formation, the only component is $G_{B;prot}$. The difference in electrostatic free energy upon complex formation is then

$$\Delta G_{el} = \Delta G_{res} + \Delta G_{prot} + \Delta G_{int1} + G_{int2} \quad (5a)$$

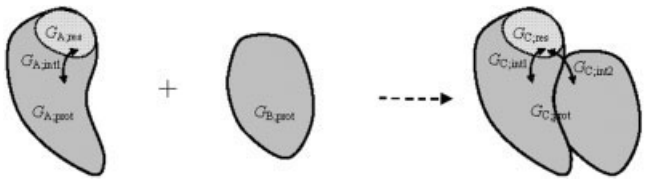

Fig. 3. Decomposition of the electrostatic free energy. The mutated residue, located on protein A, is shaded in white, whereas the rest of the protein A and the whole of protein B is shaded in gray. The energy arising solely from the charges of the mutated residue is denoted as $G_{P;res}$, where P is A (or C) before (or after) complex formation. $G_{P;prot}$ arises from the charges on either the rest of protein A when P is A, or the whole of protein B when P is B, or the rest of the protein complex when P is C. The energy of interaction between the residue and the rest of protein A is denoted as $G_{P;int1}$, where P is A (or C) before (or after) complex formation. After complex formation, there is an additional interaction between the residue and protein B, which is denoted as $G_{C;int2}$ here and just G_{int2} elsewhere.

where $\Delta G_{res} = G_{C;res} - G_{A;res}$, $\Delta G_{prot} = G_{C;prot} - G_{A;prot} - G_{B;prot}$, and $\Delta G_{int1} = G_{C;int1} - G_{A;int1}$. When the residue is mutated, the change in ΔG_{el} is

$$\delta\Delta G_{el} = \delta\Delta G_{res} + \delta\Delta G_{prot} + \delta\Delta G_{int1} + \delta\Delta_{int2} \quad (5b)$$

Note that $\delta\Delta G_{prot} = \delta G_{C;prot} - \delta G_{A;prot}$ involves only the complex and protein A, like all the other terms in Equation 5b. Thus protein B in isolation is not required for calculating $\delta\Delta G_{el}$. For a mutation that simply discharges a residue X and leaves the rest of the protein (complex) unchanged, denoted as "X → O", G_{res}, G_{int1}, and G_{int2} are zero after the mutation and G_{prot} is unchanged by the mutation, hence

$$\delta\Delta G_{el}(X \rightarrow O) = \Delta G_{res}(X) + \Delta G_{int1}(X) + G_{int2}(X) \quad (6)$$

Double Mutants and Coupling Energy

A double mutation can be viewed as two consecutive single mutations. Consider the case where the first single mutation is to change residue X on protein A into X′ and the second single mutation is to change residue Y on protein B into Y′. If the association constant is changed from K_a to K_a'', then

$$\delta\Delta G(XY \rightarrow X'Y') \equiv -k_B T \ln(K_a''/K_a) = [G_C(X'Y') - G_C(XY)] - [G_A(X') - G_A(X)] - [G_B(Y') - G_B(Y)] \quad (7a)$$

$$= [G_C(X'Y') - G_C(X'Y)] - [G_B(Y') - G_B(Y)] + [G_C(X'Y) - G_C(XY)] - [G_A(X') - G_A(X)] = \delta\Delta G(X'Y \rightarrow X'Y') + \delta\Delta G(XY \rightarrow X'Y) \quad (7b)$$

A double-mutant cycle allows for the isolation of the interaction between residues X and Y.[30] To illustrate the basic idea, let us focus on the electrostatic contribution and consider the case where the mutations are simply to discharge residues X and Y. Then the second term of Equation 7b is directly given by Equation 6. The first term can also be obtained from Equation 6, but with Y replacing X and the interaction between X and Y, G_{int}(X-Y), missing

from G_{int2}(Y). The latter is because the Y mutation is made on the neutralized X background. Consequently

$$\delta\Delta G(XY \rightarrow OO) = \delta\Delta G(XY \rightarrow XO) + \delta\Delta G(XY \rightarrow OY) - G_{int}(X - Y) \quad (8a)$$

Or

$$G_{coup}(X - Y) \equiv \delta\Delta G(XY \rightarrow OO) - \delta\Delta G(XY \rightarrow XO) - \delta\Delta G(XY \rightarrow OY) = G_{int}(X - Y) \quad (8b)$$

In practice, truly "neutralizing" mutations are impossible to make and the assumption of additivity inherent in deriving Equation 8 may not be valid. Nonetheless the coupling energy G_{coup}(X-Y) obtained from a double-mutant cycle provides the closest estimate to the interaction energy G_{int}(X-Y) between two residues. In G_{coup}(X-Y) effects from nonelectrostatic sources are also reduced to a minimum, hence a comparison of experimental and calculated G_{coup}(X-Y) offers one of the best tests of electrostatic models.

Setup of Electrostatic Calculations

The electrostatic free energy of each protein or complex was calculated from the linearized Poisson-Boltzmann equation. If the protein has N atoms with partial charges q_i, $i = 1$ to N, and the electrostatic potentials at the atoms are ϕ_i, then

$$G_{el} = \sum_{i=1}^{N} q_i\phi_i/2 \quad (9)$$

The electrostatic potential at each position is the sum of the contributions from all the charges, and each contribution is proportional to the particular partial charge. The energy of interaction between two sets of charges, 1 and 2, can be calculated from the potential arising from either set 1, denoted as $\phi_j(1)$, or from the corresponding quantity $\phi_i(2)$ arising from set 2. Specifically,

$$G_{int}(1 - 2) = \sum_{\text{set 2}} q_j\phi_j(1) = \sum_{\text{set 1}} q_i\phi_i(2) \quad (10)$$

In the first expression, the potential arising from set-1 charges is calculated at the positions of the set-2 charges, and the sum is over the set-2 charges. In the second expression, the roles of set 1 and set 2 are reversed. The identity of the two expressions can serve as an important check on numerical accuracy.

The electrostatic free energy can be decomposed into a Coulombic term, obtained when the protein dielectric (with dielectric constant ϵ_p) is extended to infinity, and a solvation term, when the solvent dielectric is accounted for:

$$G_{el} = G_{Coul} + G_{solv} \quad (11)$$

For a set of charges q_i, the Coulomb term is

$$G_{Coul} = 166\sum_{i \neq j} q_i q_j / \epsilon_p r_{ij} \quad (12)$$

where r_{ij} is the distance between charges q_i and q_j in Ångstroms and the resulting energy is in kcal/mol. To maximize cancellation of numerical errors, the Poisson-Boltzmann equation was solved twice, once with the actual solvent dielectric and once with the protein dielectric extended to infinity. The difference in energy between these two calculations gave G_{solv}. The Coulomb term, calculated according to Equation 12, was then added when necessary.

An explanation for how each of the four terms in Equation 5b was calculated is in order. ΔG_{res} was calculated with the residue under mutation charged but the rest of the protein or protein complex uncharged. The Coulomb term of G_{res} is exactly the same before and after complex formation and hence was not needed. For ΔG_{prot}, again only the solvation term, obtained with the protein or protein complex charged but the residue uncharged, was needed, since the Coulomb term is not changed by mutation. The energy of interaction between the residue and the rest of the protein or protein complex was calculated by either charging the residue or charging the rest of the protein or protein complex. The two ways gave nearly identical results. The resulting $\delta\Delta G_{el}$ from this decomposition procedure was also checked against that calculated according to Equation (3). In the latter method, the overall electrostatic contribution ΔG_{el} was calculated before and after the mutation, and the difference gave $\delta\Delta G_{el}$. The two methods gave very close results.

Once the potential of the mutated residue was calculated, further decomposition of the interaction energy was easily done. For example, the decomposition of the interaction energy in the complex into $G_{C;int1}$ and G_{int2} was accomplished by multiplying the potential from the mutated residue with the charges of protein A and protein B, respectively, in the complex. Contributions to $G_{C;int1}$ and G_{int2} from interactions with individual residues, on protein A and on protein B, respectively, could also be obtained by multiplying the potential with the charges of those residues. For interactions with protein A residues, the net contribution to binding stability is given by $\Delta G_{int1} = G_{C;int1} - G_{A;int1}$, which was obtained by calculating the potential of the mutated residue twice, once with the residue within protein A only and once with the residue within the complex.

The Poisson-Boltzmann equation was solved using the UHBD program.[24] Details are listed in Table II. Three protocols were tested. In the first, denoted as vdw4, the dielectric boundary between the protein and the solvent was defined as the van der Waals surface of the protein and the protein dielectric constant was assigned a low value of 4. In the other two protocols, the dielectric boundary was defined as the commonly used molecular surface. This surface, denoted as SE, is the surface from which a spherical solvent probe with a 1.4-Å radius is excluded from the protein interior. The protein dielectric constant was then assigned a value of either 4 or 20, leading to protocols SE4 and SE20. The relatively high value of 20 was originally used by Antosiewicz et al.[31] in pK_a calculations.

TABLE II. Setup of Electrostatic Calculations

	Solvent conditions[a]			ΔG_{el} (kcal/mol)[c]		
Complex	I (mM)	T (K)	Discretization[b]	vdW4	SE4	SE20
IL4:IL4BP	150	298	100 → 140 → 140	−14.8	−4.6	−8.5
FKBP:CN	100	303	100 → 160 → 200	0.7	26.5	3.7
Rap1 A:Raf1	65	300	100 → 140 → 140	−8.7	0.5	−5.2
CD2:CD58	100	298	100 → 140 → 140	−7.6	16.9	−2.9
Im9:E9	225	298	100 → 140 → 140	−8.0	4.5	−4.4
AChE:Fas	100	298	100 → 180 → 240	−9.1	9.7	−4.7

[a]Solvent conditions were matched to those in experimental studies. The solvent dielectric constant ε_s was set to the value of water at the selected temperature (e.g., 78.5 at 298 K and 76.6 at 303 K).
[b]Discretization for PB calculations had the same dimension along the three Cartesian coordinates. First a course grid, with a dimension of 100 in each direction and a grid size of 1.5 Å, was centered at the geometric center of each complex. This grid was large enough so that boundary effects can be neglected. Then a finer grid, with a dimension of 140, 160, or 180 in each direction and a grid size of 0.7 Å, was placed at the same center. This grid was large enough to cover the entire complex. The boundary conditions were calculated from the results on the course grid. An even finer grid, with a dimension of 140, 200, or 240 in each direction and a grid size of 0.25 Å, was centered on the CB atom of the residue (or CA in the case of a Gly residue) to be mutated.
[c]The three protocols differ in the specification of the dielectric boundary (vdW or SE) and the value of the protein dielectric constant (4 or 20).

The PDB entries used for the six protein complexes studied are listed in Table I. Onto each PDB, hydrogens were added to all heavy atoms and energy-minimized in the InsightII program (version 2000, Accelrys, San Diego, CA). Mutation was modeled by replacing the side chain and energy-minimizing its conformation. The subunits of the wild-type or mutant complex were then separated into protein A and protein B. For the Poisson-Boltzmann calculations, protein charges were from the Amber force field[32] and the radii were adapted from OPLS[33] and Bondi radii.[34] Specifically, the radii of carbon, hydrogen, nitrogen, oxygen, and sulfur were 1.9, 1.2, 1.625, 1.48, and 1.775 Å, respectively. Arginine and lysine residues were taken to be positively charged and aspartate and glutamate residues were taken to be negatively charged; all other residues were neutral. pK_as of ionizable groups may shift upon complex formation and thus changes in ionization states could affect binding stability; this effect was not considered in the present study. Solvent temperature and ionic strength, listed in Table II, were selected to match experimental conditions.

Area of solvent accessibility (ASA) was calculated using the DSSP program.[35] van der Waals interaction energy ΔG_{vdW} between the proteins in a complex was calculated with parameters in the Amber force field.[32]

Collection of Mutations

Our focus was on mutations that could have dominant electrostatic contributions to the change in binding stability. Therefore all substitutions between nonpolar residues were not considered. Other cases not considered were alanine mutations of polar residues in which the polar groups (such as the hydroxyl of tyrosine) are not in direct interactions with the partner protein, with the exception of Raf1_Q66A, which was retained as a counter example. For the IL4:IL4BP complex, our study included 12 single mutations in Table 3 of Zhang et al.[7] (see Table III). In addition, six double mutants were studied to assess the calculation of coupling energy (also listed in Table III). For the FKBP:CN complex, 14 single mutations from Table I of Yang et al.[9] and Table I of Futer et al.[10] were studied (see Table IV). For the Rap1A:Raf1 complex, our study included 13 single mutations from the work of Nassar et al.[11] (listed in Table V). For the CD2:CD58 complex, 10 single mutations from the work of Kim et al.[12] were studied (see Table VI). For the Im9:E9 complex, our study included five single mutations that were found by Wallis et al.[13] to affect the binding stability by more than 1 kcal/mol (see Table VII). For the AChE:Fas complex, four single mutations from Table III of Radic et al.[15] were studied (see Table VIII). In total, our study covered 64 mutations on the six protein complexes.

RESULTS

Overall Electrostatic Contribution to Binding Stability

The net charges of the proteins of the six complexes are listed in Table I. In all but one complexes, the proteins have opposite charges. The exception is the CD2:CD58 complex, in which both proteins carry a small net negative charge. The net charge on FKBP is also small.

The overall electrostatic contributions to the binding stability of the six complexes are listed in Table II. As found previously on the barnase:barstar complex,[2] the vdW4 and SE20 protocols gave qualitatively similar results. They predicted favorable electrostatic contributions for five of the complexes, including the CD2:CD58 complex with like-charge partners. For the FKBP:CN complex, vdW4 and SE20 predicted a net unfavorable electrostatic contribution. On the other hand, SE4 predicted unfavorable electrostatic contributions for five of the six complexes. That the predicted contributions by vdW4 and SE20 were favorable for like-charge partners CD2 and CD58 and unfavorable for opposite-charge partners FKBP and CN indicate that the distributions of charges, not just the net charges, are important for electrostatic contribution. In particular, charges around the interface are likely to make far greater contributions to binding than those away from the interface. That vdW4 and SE4 predicted opposite overall electrostatic contributions in four of the six complexes indicate sensitivity of calculated results on the specification of the dielectric boundary.

TABLE III. Effects of Mutations on the Stability of the IL4-IL4BP Complex[a]

		Energetic decomposition				Interactions[b]	
Protocol	$\delta\Delta G_{el}$	$\delta\Delta G_{res}$	$\delta\Delta G_{prot}$	$\delta\Delta G_{int1}$	δG_{int2}	Energy (kcal/mol)	Distance (Å)
			IL4_E9Q ($\delta\Delta G_{exp}$ = 3.0; $\delta\Delta$ASA = 0)				
vdW4	2.98	−2.58	0.22	2.32	3.02	IL4_K12: 1.4	OE2-NZ: 4.9
SE4	7.10	−10.3	−0.04	8.10	9.36	IL4BP_Y13: 1.4	OE2-OH: 2.9
SE20	1.12	−1.61	−0.01	1.66	1.08	IL4BP_S70: 1.3	OE1-N: 2.8
						IL4BP_Y183: 1.1	OE2-OH: 2.7
			IL4_T13A ($\delta\Delta G_{exp}$ = 1.0; $\delta\Delta$ASA = 17)				
vdW4	0.60	−0.11	0.03	0.10	0.58	IL4BP_Y127: 0.7	OG1-OH: 2.6
SE4	1.05	−0.22	0.21	−0.06	1.12		
SE20	0.22	−0.03	0.03	0.02	0.20		
			IL4_R53A ($\delta\Delta G_{exp}$ = 1.7; $\delta\Delta$ASA = −58)				
vdW4	0.25	−0.52	−0.13	0.78	0.12	IL4_D87: 1.1	NH2-ODI: 2.9
SE4	1.36	−2.77	−0.61	4.94	−0.20		
SE20	0.37	−0.43	0.00	0.48	0.32		
			IL4_R88A ($\delta\Delta G_{exp}$ = 3.9; $\delta\Delta$ASA = −119)				
vdW4	4.18	−1.32	−0.68	−0.24	6.42	IL4BP_D67: 1.4	NH2-OD2: 5.3
SE4	4.62	−4.72	−3.56	−0.44	12.46	IL4BP_D72: 5.0	NH2-OD2: 2.9
SE20	2.83	−0.98	−0.35	−0.10	4.26		
			IL4_N89A ($\delta\Delta G_{exp}$ = 1.4; $\delta\Delta$ASA = 15)				
vdW4	0.38	−0.22	−0.12	0.12	0.60		
SE4	1.31	−0.72	0.55	0.30	1.18		
SE20	0.28	−0.11	0.11	0.02	0.26		
			IL4BP_Y13F ($\delta\Delta G_{exp}$ = 1.9; $\delta\Delta$ASA = 2)				
vdW4	0.66	−0.10	−0.24	0.02	0.98	IL4_E9: 1.2	OH-OE2: 2.9
SE4	1.80	−0.05	0.01	−0.92	2.76		
SE20	0.36	0.00	0.00	0.00	0.36		
			IL4BP_D67A ($\delta\Delta G_{exp}$ = 2.3; $\delta\Delta$ASA = −51)				
vdW4	4.38	−1.17	−0.38	−1.02	6.96	IL4_R81: 1.5	OD1-NH2: 3.8
SE4	6.17	−5.5	−0.97	−2.08	14.72	IL4_R85: 4.1	OD2-NE: 2.9
SE20	3.52	−1.07	−0.09	−0.38	5.06	IL4_R88: 1.5	OD2-NH2: 5.3
						IL4BP_D72: −0.5	OD1-OD2: 7.2
			IL4BP_D72A ($\delta\Delta G_{exp}$ = 4.3; $\delta\Delta$ASA = −19)				
vdW4	3.83	−1.31	−0.38	−0.02	5.54	IL4_R88: 5.3	OD2-NH2: 2.7
SE4	7.02	−5.30	0.22	1.22	10.88		
SE20	2.69	−0.87	0.04	0.00	3.52		
			IL4BP_D72N ($\delta\Delta G_{exp}$ = 4.5; $\delta\Delta$ASA = 4)				
vdW4	3.01	−1.13	0.20	−0.10	4.04	IL4_R88: 3.7	OD2-NH2: 2.7
SE4	4.62	−4.85	0.17	0.88	8.42		
SE20	2.15	−0.81	0.00	−0.04	3.00		
			IL4BP_Y127A ($\delta\Delta G_{exp}$ = 2.2; $\delta\Delta$ASA = −101)				
vdW4	0.32	−0.18	−0.32	0.00	0.82	IL4_T13: 0.7	OH-OG1: 2.6
SE4	−0.05	−0.75	−1.06	−0.02	1.78		
SE20	0.21	−0.11	−0.06	0.00	0.38		
			IL4BP_Y183A ($\delta\Delta G_{exp}$ = 3.7; $\delta\Delta$ASA = −16)				
vdW4	1.29	−0.24	−0.75	−0.08	2.36	IL4_E9: 1.9	OH-OE2: 2.7
SE4	1.13	−0.52	−3.21	−0.32	5.18		
SE20	0.51	−0.06	−0.43	−0.04	1.04		
			IL4BP_Y183F ($\delta\Delta G_{exp}$ = 3.2; $\delta\Delta$ASA = 2)				
vdW4	1.46	−0.22	−0.50	−0.06	2.24	IL4_E9: 1.8	OH-OE2: 2.7
SE4	4.02	−0.14	−0.38	−0.28	4.82		
SE20	0.87	−0.02	−0.05	−0.04	0.98		
			IL4_E9Q/IL4BP_Y13F ($\delta\Delta G_{exp}$ = 4.3; $\delta\Delta$ASA = 3)				
vdW4	2.38	−2.74	0.16	2.00	2.96		
SE4	6.35	−10.34	0.09	8.02	8.58		
SE20	0.93	−1.61	0.00	1.66	0.88		

Comparison of Calculated $\delta\Delta G_{el}$ and Experimental $\delta\Delta G$

Of the 64 mutations, eight had experimental $\delta\Delta G$ totally different from predicted $\delta\Delta G_{el}$ by all three calculation protocols. These will be further discussed later. Another mutation, Raf1_Q66A, was included as an example of mutation on a polar residue in which the polar groups are not in direct interaction with the partner protein [Fig.

TABLE III. Continued

Protocol	$\delta\Delta G_{el}$	Energetic decomposition				Interactions[b]	
		$\delta\Delta G_{res}$	$\delta\Delta G_{prot}$	$\delta\Delta G_{int1}$	δG_{int2}	Energy (kcal/mol)	Distance (Å)
IL4_E9Q/IL4BP_Y183A ($\delta\Delta G_{exp}$ = 5.5; $\delta\Delta$ASA = −17)							
vdW4	3.20	−2.85	−0.43	2.18	4.30		
SE4	5.20	−10.84	−3.64	7.78	11.90		
SE20	1.09	−1.67	−0.46	1.62	1.60		
IL4_E9Q/IL4BP_Y183F ($\delta\Delta G_{exp}$ = 5.0; $\delta\Delta$ASA = 6)							
vdW4	3.63	−2.84	−0.03	2.18	4.32		
SE4	8.80	−10.47	−0.69	7.76	12.20		
SE20	1.56	−1.63	−0.07	1.62	1.64		
IL4_T13A/IL4BP_Y127A ($\delta\Delta G_{exp}$ = 2.5; $\delta\Delta$ASA = −100)							
vdW4	0.37	−0.21	−0.22	0.12	0.68		
SE4	−0.08	−0.90	−0.78	−0.08	1.68		
SE20	0.21	−0.13	0.34	−0.32	0.32		
IL4_R88A/IL4BP_D72A ($\delta\Delta G_{exp}$ = 5.3; $\delta\Delta$ASA = −130)							
vdW4	3.95	−1.71	−0.66	−0.54	6.86		
SE4	2.78	−6.22	−3.62	0.24	12.38		
SE20	2.61	−1.36	−0.35	0.36	4.68		
IL4_R88A/IL4BP_D72N ($\delta\Delta G_{exp}$ = 4.7; $\delta\Delta$ASA = −118)							
vdW4	4.07	−1.54	−0.63	−0.68	6.92		
SE4	2.70	−5.94	−3.52	−0.28	12.44		
SE20	2.57	−1.33	−0.36	−0.46	4.72		

[a]The list of mutations is from Table 3 of Zhang et al.[7] All energies are in kcal/mol, distances in Å, and mutational changes in buried area of solvent accessibility ($\delta\Delta$ASA) in Å^2.

[b]Changes in interaction energies calculated by the vdW protocol are listed. Interaction refers to that between the residue under mutation and another residue on either the same subunit or the other subunit. The contribution of a residue pair to $\delta\Delta G_{int1}$ or δG_{int2} is listed if the magnitude is greater than 1.0 kcal/mol. If no such partner residue is found, then the energy cutoff is lowered to 0.5 kcal/mol. Positive values indicate that the interactions are more favorable in the wild-type complex. For each residue pair, the atoms with the closest polar contact and the contact distance in the wild-type complex are also listed.

1(d)]. In this case all three calculation protocols predicted minimal electrostatic effect for the mutation, compared to a 1.6 kcal/mol destabilization found experimentally (Table V). For the remaining 55 mutations, comparison of experimental $\delta\Delta G$ and predicted $\delta\Delta G_{el}$ are shown in Figure 4(a–c) for the three calculation protocols. Among the three protocols, vdW4 showed the closest agreement with experimental data, but even for this protocol the root-mean-square-deviation (RMSD) was as large as 1.46 kcal/mol. In comparison, the RMSDs of the SE4 and SE20 predictions were 2.03, and 1.82 kcal/mol, respectively. The relative performance of the three protocols found here on the large set of mutations is in agreement with what was found in previous studies on the barnase:barstar complex.[2,36]The electrostatic calculations by the vdW4 protocol appear to systematically underestimate the destabilizing effects of the mutants. Out of the 55 mutations, $\delta\Delta G_{el}$ < experimental $\delta\Delta G$ in 37 cases. The underestimation was also seen in a previous study on the barnase:barstar complex,[2] where it was attributed to the neglect of hydrophobic and van der Waals interaction. This possibility will be further investigated below.

Comparison of Calculated and Experimental Coupling Energies

Six double mutations on the IL4:IL4BP complex were studied to test the calculation of coupling energy. These six, IL4_E9Q/IL4BP_Y13F, IL4_E9Q/IL4BP_Y183A, IL4_E9Q/IL4BP_Y183F, IL4_T13A/IL4BP_Y127A, IL4_R88A/IL4BP_D72A, and IL4_R88A/IL4BP_D72N, are among the double mutants that Zhang et al.[7] found to have the highest coupling energies in magnitude. Comparison against experimental data is shown in Figure 5 for the three calculation protocols. vdW4 again showed the best agreement with experiment. Overall SE4 overestimated the magnitudes of coupling energies whereas SE20 underestimated them.

Decomposition of $\delta\Delta G_{el}$

Decomposition of $\delta\Delta G_{el}$ according to Equation 5b further highlights the differences among the three calculation protocols. As Tables III–VIII show, of the four terms, $\delta\Delta G_{prot}$, the effect of mutation on the desolvation cost of the rest of the protein, is quite small, as expected. $\delta\Delta G_{prot}$ vanishes for an idealized "X → O" mutation, which simply discharges a residue X. In general, SE4 yielded large magnitudes for both the residue desolvation cost $\delta\Delta G_{res}$ and the interaction terms $\delta\Delta G_{int1}$ and δG_{int2}. For example, for the IL4_E9Q mutation on the IL4:IL4BP complex, the values of $\delta\Delta G_{res}$, $\delta\Delta G_{int1}$, and δG_{int2} according to SE4 were −10.3, 8.1, and 9.4 kcal/mol, respectively, resulting a destabilizing effect of 7.1 kcal/mol. In comparison, the three terms according to vdW4 were −2.6, 2.3, and 3.0 kcal/mol, respectively. The contrast between SE4 and vdW4 is explained by the less solvent exposure of protein charges in the former protocol, in which crevices not accessible to a 1.4-Å solvent probe are assigned to the protein dielectric. The large magnitudes of $\delta\Delta G_{int1}$ in the SE4 calculations lead to the overestimated magnitudes of cou-

TABLE IV. Effects of Mutations on the Stability of the FKBP:CN Complex[a]

		Energetic decomposition				Interactions[b]	
Protocol	$\delta\Delta G_{el}$	$\delta\Delta G_{res}$	$\delta\Delta G_{prot}$	$\delta\Delta G_{int1}$	δG_{int2}	Energy (kcal/mol)	Distance (Å)
			FKBP_K35I ($\delta\Delta G_{exp}$ = 0.0; $\delta\Delta$ASA = 14)				
vdW4	3.83	−1.57	−0.48	1.54	4.34	FKBP_D41: 1.9	NZ-OD1: 2.7
SE4	7.86	−5.65	−0.81	5.66	8.66	CNA_L312: 1.1	NZ-O: 2.7
SE20	3.13	−1.08	−0.09	1.10	3.20	CNA_D313: 1.7	NZ-OD2: 5.3
			FKBP_D37V ($\delta\Delta G_{exp}$ = 3.2; $\delta\Delta$ASA = 3)				
vdW4	−0.90	−0.70	0.02	1.48	−1.70	FKBP_D41: −1.0	OD1-OD2: 4.0
SE4	−0.30	−4.57	4.10	2.91	−2.74	FKBP_R42: 1.4	OD1-NH1: 3.1
SE20	−0.85	−0.69	0.02	1.20	−1.38		
			FKBP_R40A ($\delta\Delta G_{exp}$ = 0.0; $\delta\Delta$ASA = −28)				
vdW4	0.68	−0.25	−0.43	0.22	1.14		
SE4	0.68	−0.76	−0.42	0.34	1.52		
SE20	0.95	−0.20	0.01	0.16	0.98		
			FKBP_R42A ($\delta\Delta G_{exp}$ = 2.1; $\delta\Delta$ASA = −42)				
vdW4	1.96	−1.08	−0.18	1.28	1.94	FKBP_D37: 1.2	NH1-OD1: 3.1
SE4	3.93	−5.50	−0.35	5.22	4.56		
SE20	1.67	−0.80	0.03	1.02	1.48		
			FKBP_R42I ($\delta\Delta G_{exp}$ = 3.1; $\delta\Delta$ASA = −17)				
vdW4	2.38	−1.06	0.20	1.28	1.88	FKBP_D37: 1.2	NH1-OD1: 3.1
SE4	4.21	−5.54	−0.17	5.30	4.62		
SE20	1.80	−0.80	0.08	1.04	1.48		
			FKBP_R42K ($\delta\Delta G_{exp}$ = 2.8; $\delta\Delta$ASA = −12)				
vdW4	−0.30	0.36	−0.18	−0.38	−0.10		
SE4	−0.64	1.74	−0.76	−1.18	−0.44		
SE20	−0.07	0.31	−0.06	−0.34	0.02		
			FKBP_R42Q ($\delta\Delta G_{exp}$ = 2.5 to 2.8; $\delta\Delta$ASA = −13)				
vdW4	1.88	−0.99	−0.15	1.14	1.88	FKBP_D37: 1.1	NH1:OD1: 3.1
SE4	3.99	−4.97	−0.38	4.70	4.64		
SE20	1.71	−0.72	0.01	0.94	1.48		
			FKBP_K44A ($\delta\Delta G_{exp}$ = −1.2; $\delta\Delta$ASA = −115)				
vdW4	0.17	−0.84	−0.27	0.06	1.22	CNB_N121: 1.40	NZ-OD1: 2.6
SE4	−1.26	−2.62	−0.4	−0.18	1.94		
SE20	−0.05	−0.6	−0.07	0.14	0.48		
			FKBP_Q53A ($\delta\Delta G_{exp}$ = −0.3; $\delta\Delta$ASA = −94)				
vdW4	−0.20	0.00	−0.26	0.02	0.04		
SE4	−1.76	−0.20	−1.66	0.02	0.08		
SE20	−0.29	−0.03	−0.32	0.04	0.02		
			FKBP_H87A ($\delta\Delta G_{exp}$ = 0.0 to −0.6; $\delta\Delta$ASA = −64)				
vdW4	0.28	−0.07	0.01	0.12	0.22		
SE4	−0.36	−0.47	−0.49	0.20	0.40		
SE20	0.02	−0.05	−0.11	0.04	0.14		
			FKBP_H87F ($\delta\Delta G_{exp}$ = 0.4; $\delta\Delta$ASA = 16)				
vdW4	0.19	−0.03	0.06	0.10	0.06		
SE4	−0.28	−0.31	−0.11	0.10	0.04		
SE20	0.01	0.04	−0.03	0.04	0.04		
			FKBP_H87L ($\delta\Delta G_{exp}$ = 0.3; $\delta\Delta$ASA = −37)				
vdW4	0.25	−0.07	0.02	0.10	0.20		
SE4	−0.30	−0.49	−0.35	0.18	0.36		
SE20	0.07	−0.05	−0.06	0.04	0.14		
			FKBP_H87V ($\delta\Delta G_{exp}$ = 0.9; $\delta\Delta$ASA = −52)				
vdW4	0.18	−0.07	−0.07	0.10	0.22		
SE4	−0.35	−0.49	−0.42	0.20	0.36		
SE20	0.07	−0.05	−0.06	0.04	0.14		
			FKBP_I90K ($\delta\Delta G_{exp}$ = 2.7 to 4.7; $\delta\Delta$ASA = 28)				
vdW4	0.84	2.70	0.02	−0.10	−1.78	CNA_D348: −1.3	NZ-OD1: 8.6
SE4	5.31	10.23	−0.26	−0.94	−3.72		
SE20	−0.13	1.52	−0.03	−0.04	−1.58		

[a]The list of mutations is from Table 1 of Yang et al.[9] and Table 1 of Futer et al.[10]

TABLE V. Effects of Mutations on the Stability of the Rap1A:Raf1 Complex[a]

		Energetic decomposition				Interactions[b]	
Protocol	$\delta\Delta G_{el}$	$\delta\Delta G_{res}$	$\delta\Delta G_{prot}$	$\delta\Delta G_{int1}$	δG_{int2}	Energy	Distance
			Raf1_R59A ($\delta\Delta G_{exp} = 1.9$; $\delta\Delta ASA = -33$)				
vdW4	2.36	−0.47	−0.57	−0.38	3.78	Rap1A_E37: 3.1	NH1-OE1: 3.0
SE4	3.06	−1.04	−1.62	−0.88	6.60		
SE20	1.90	−0.23	−0.23	−0.36	2.72		
			Raf1_N64A ($\delta\Delta G_{exp} = 0.5$; $\delta\Delta ASA = -56$)				
vdW4	0.26	−0.06	−0.20	−0.02	0.54	Rap1A_R41: 0.5	OD1-NH2: 2.9
SE4	0.12	−0.28	−0.66	−0.06	1.12		
SE20	0.15	−0.05	−0.10	−0.02	0.32		
			Raf1_N64D ($\delta\Delta G_{exp} = 1.5$; $\delta\Delta ASA = -20$)				
vdW4	−0.87	0.75	0.00	−0.20	−1.42	Rap1A_R41: −2.0	OD1-NH2: 2.9
SE4	−0.93	2.46	−0.27	−0.20	−2.92		
SE20	−0.52	0.51	−0.05	−0.20	−0.78		
			Raf1_K65A ($\delta\Delta G_{exp} = 1.1$; $\delta\Delta ASA = -47$)				
vdW4	−0.40	−0.11	−0.07	−0.08	−0.14	Rap1A_E3: 0.8	NZ-OE1: 4.8
SE4	−1.38	−0.55	−0.41	−0.14	−0.28	Rap1A_R41: −0.9	NZ-NH1: 4.6
SE20	−0.42	−0.15	−0.07	−0.06	−0.14	Rap1A_E54: 0.5	NZ-OE1:8.1
			Raf1_K65E ($\delta\Delta G_{exp} = 0.9$; $\delta\Delta ASA = 4$)				
vdW4	−0.46	0.24	0.02	−0.28	−0.44	Rap1A_E3: 1.6	NZ-OE1: 4.8
SE4	−0.65	0.91	−0.02	−0.26	−1.28	Rap1A_K5: −1.1	NZ-NZ: 8.6
SE20	−0.45	0.20	−0.01	−0.16	−0.48	Rap1A_R41: −2.2	NZ-NH1: 4.6
						Rap1A_E54: 1.2	NZ-OE1: 8.1
			Raf1_K65M ($\delta\Delta G_{exp} = 0.7$; $\delta\Delta ASA = -19$)				
vdW4	−0.35	−0.11	0.00	−0.10	−0.14	Rap1A_E3: 0.9	NZ-OE1: 4.8
SE4	−1.20	−0.54	−0.18	−0.16	−0.32	Rap1A_K5: −0.5	NZ-NZ: 8.6
SE20	−0.40	−0.15	−0.03	−0.08	−0.14	Rap1A_R41: −1.0	NZ-NH1: 4.6
						Rap1A_E54: 0.5	NZ-OE1: 8.1
			Raf1_Q66A ($\delta\Delta G_{exp} = 1.6$; $\delta\Delta ASA = -29$)				
vdW4	−0.02	−0.07	−0.09	−0.15	0.06		
SE4	0.03	−0.42	−0.15	−0.27	0.12		
SE20	0.01	−0.07	0.00	0.00	0.00		
			Raf1_R67A ($\delta\Delta G_{exp} = 1.5$; $\delta\Delta ASA = -113$)				
vdW4	1.20	−0.47	−0.33	−0.36	2.36	Rap1A_E37: 1.4	NH1-OE2: 4.1
SE4	−0.93	−2.25	−1.90	−1.40	4.62	Rap1A_E54: 1.3	NH2-OE2: 3.7
SE20	0.94	−0.54	−0.26	−0.38	2.12		
			Raf1_T68A ($\delta\Delta G_{exp} = 1.5$; $\delta\Delta ASA = -2$)				
vdW4	0.85	−0.12	−0.25	−0.16	1.38	Rap1A_D38:1.3	OG1-OD1: 2.7
SE4	1.37	−0.18	−0.19	−0.38	2.12		
SE20	0.31	−0.02	−0.01	−0.10	0.44		
			Raf1_K84A ($\delta\Delta G_{exp} = 1.3$; $\delta\Delta ASA = -60$)				
vdW4	2.12	−0.41	−0.37	−0.62	3.52	Rap1A_D33: 2.7	NZ-OD2: 2.9
SE4	2.33	−1.15	−1.38	−1.12	5.98	Rap1A_D38: 1.0	NZ-OD2: 8.8
SE20	1.50	−0.29	−0.25	−0.44	2.48		
			Raf1_K84E ($\delta\Delta G_{exp} = 2.2$; $\delta\Delta ASA = -19$)				
vdW4	2.65	−0.26	−0.35	−1.06	4.32	Rap1A_K31: −1.0	NZ-NZ: 8.5
SE4	3.52	−0.80	−1.18	0.26	5.24	Rap1A_D33: 3.4	NZ-OD2: 2.9
SE20	2.10	−0.14	−0.20	−0.78	3.22	Rap1A_D38: 1.5	NZ-OD2: 8.8
			Raf1_R89L ($\delta\Delta G_{exp} > 2.6$; $\delta\Delta ASA = 7$)				
vdW4	3.63	−1.79	−0.34	−0.30	6.06	Rap1A_D38: 3.4	NH2-OD1: 2.9
SE4	6.08	−6.17	−0.61	−0.48	13.34	Rap1A_S39: 1.2	NH2-OG: 5.3
SE20	2.68	−1.00	−0.06	−0.22	3.98	Rap1A_D57: 1.0	NH2-OD2: 7.2
			Rap1A_K31E ($\delta\Delta G_{exp} = -1.8$; $\delta\Delta ASA = 57$)				
vdW4	−2.08	0.16	0.00	0.84	−3.10	Raf1_K84: −1.4	NZ-NZ: 8.5
SE4	−1.54	0.96	0.06	1.34	−3.90		
SE20	−1.93	0.22	0.01	0.68	−2.84		

[a]The list of mutations is from Table 2 of Nassar et al.[11]

pling energies noted earlier. From here on, unless otherwise indicated, calculation results will refer to those obtained by the vdW4 protocol.Tables III–VIII also list the effects of mutations on the interaction energies of mutated residues with other individual residues. The interactions sometimes had magnitudes over 3 kcal/mol, e.g., between IL4_R85 and

TABLE VI. Effects of Mutations on the Stability of the CD2:CD58 Complex[a]

		Energetic decomposition				Interactions[b]	
Protocol	$\delta\Delta G_{el}$	$\delta\Delta G_{res}$	$\delta\Delta G_{prot}$	$\delta\Delta G_{int1}$	δG_{int2}	Energy	Distance
			CD2_D31A ($\delta\Delta G_{exp} > 2.3$; $\delta\Delta ASA = 5$)				
vdW4	1.86	−0.51	−0.05	1.06	1.36	CD2_R48: 1.0	OD1-NE: 3.1
SE4	2.58	−3.11	−1.23	2.50	4.42	CD58_K34: 1.8	OD2-NZ: 5.5
SE20	0.93	−0.56	−0.13	0.78	0.84	CD58_E37: −1.2	OD2-OE2: 6.1
						CD58_R44: 2.2	OD2-NH1: 3.1
			CD2_D32A ($\delta\Delta G_{exp} > 2.9$; $\delta\Delta ASA = 3$)				
vdW4	0.67	−0.62	−0.13	2.02	−0.60	CD58_K29: 1.0	OD2-NZ: 8.3
SE4	3.16	−2.68	−1.68	5.46	2.06	CD58_K34: 3.1	OD2-NZ: 3.2
SE20	−0.57	−0.48	−0.13	1.34	−0.16	CD58_E37: −1.5	OD2-OE1: 4.9
						CD58_E39: −1.1	OD1-OE1: 6.3
			CD2_K34A ($\delta\Delta G_{exp} > 2.3$; $\delta\Delta ASA = -41$)				
vdW4	0.96	−0.73	0.01	0.44	1.24	CD58_E25: 1.0	NZ-OE1: 7.8
SE4	−1.80	−3.98	−1.04	1.20	2.02	CD58_K29: −1.7	NZ-NZ: 5.2
SE20	0.36	−0.82	−0.16	0.38	0.96	CD58_K34: −1.6	NZ-NZ: 6.5
						CD58_E37: 1.0	NZ-OE1: 7.6
						CD58_E78: 1.8	NZ-OE1: 4.0
			CD2_K41A ($\delta\Delta G_{exp} = 1.5$; $\delta\Delta ASA = -140$)				
vdW4	−1.46	−1.81	−0.13	−0.42	0.90	CD58_K29: −0.5	NZ-OE1: 10.3
SE4	−6.09	−5.68	−0.85	−0.76	1.20	CD58_E76: 0.7	NZ-OE2: 6.3
SE20	0.00	−1.05	−0.15	−0.34	1.54	CD58_E78: 0.8	NZ-OE1: 6.8
						CD58_S85: −0.6	NZ-OG: 4.6
			CD2_K43A ($\delta\Delta G_{exp} > 2.5$; $\delta\Delta ASA = -60$)				
vdW4	2.34	−0.48	−0.22	−0.56	3.60	CD58_E25: 2.1	NZ-OE2:3.3
SE4	2.02	−1.84	−1.52	−0.98	6.36	CD58_K34: −1.0	NZ-NZ: 9.0
SE20	1.93	−0.44	−0.23	−0.46	3.06	CD85_E39: 1.0	NZ-OE1: 6.6
			CD2_R48A ($\delta\Delta G_{exp} > 2.4$; $\delta\Delta ASA = -43$)				
vdW4	3.47	−2.09	−0.76	0.26	6.06	CD58_K34: −2.2	NH2-NZ: 2.3
SE4	2.51	−7.07	−2.64	2.58	9.64	CD58_E37: 6.8	NH2-OE1: 2.7
SE20	1.81	−1.24	−0.21	0.28	2.98	CD58_E39: 1.8	NH1-OE1: 3.5
						CD58_R44: −1.5	NH1-NH1: 4.2
			CD2_K51A ($\delta\Delta G_{exp} = 1.4$; $\delta\Delta ASA = -90$)				
vdW4	5.10	−1.51	−1.11	−0.08	7.80	CD58_E37: 1.0	NZ-OE1: 6.8
SE4	5.24	−3.88	−2.64	−0.74	12.50	CD58_E39: 3.6	NZ-OE2: 2.8
SE20	3.06	−0.79	−0.41	−0.02	4.28	CD58_E42: 4.6	NZ-OE1: 2.5
			CD2_Y86F ($\delta\Delta G_{exp} = 0.8$; $\delta\Delta ASA = 1$)				
vdW4	0.45	0.01	−0.14	−0.28	0.58	CD58_K29: 0.7	OH-NZ: 2.8
SE4	0.99	−0.03	−0.02	0.14	0.90		
SE20	0.22	−0.01	0.01	0.04	0.18		
			CD2_N92A ($\delta\Delta G_{exp} = 1.0$; $\delta\Delta ASA = 4$)				
vdW4	0.76	−0.24	−0.10	−0.02	1.02	CD58_K32: 0.9	OD1-NZ: 6.0
SE4	1.34	−0.34	0.18	−0.10	1.60		
SE20	0.38	−0.04	0.04	0.02	0.36		
			CD2_E95A ($\delta\Delta G_{exp} = 0.7$; $\delta\Delta ASA = -32$)				
vdW4	1.44	−0.42	−0.20	0.52	1.54	CD58_K32: 2.0	OE2-NZ: 3.3
SE4	1.25	−2.29	−1.28	1.22	3.60	CD58_K29: 1.2	OE1-NZ: 5.7
SE20	1.08	−0.47	−0.09	0.36	1.38		

[a]The list of mutations is from Table 1 of Kim et al.[12]

IL4BP_D67, between IL4_R88 and IL4BP_D72, between Rap1A_E37 and Raf1_R59, between Rap1A_D38 and Raf1_R89, between CD2_D32 and CD58_K34, between CD2_R48 and CD58_E37, between CD2_K51 and CD58_E39 as well as CD58_E42, and between IM9_E30 and E9_R54. These pairs all form good salt bridges. As the distances between interacting residues increased, the magnitudes of their interactions progressively weakened.

In eight of the total of 64 mutations studied, the predicted $\delta\Delta G_{el}$ by none of the three protocols was compatible with experimental data. For FKBP_K35I, a large destabilization, ranging from 3.1 to 7.8 kcal/mol, was predicted. The prediction could be rationalized by a number of favorable interactions of FKBP_K35, including with the backbone carbonyl of CNA_L312 and the side-chain carboxyl of CNA_D313. However, experimentally the FKBP_K35I mutation was not found to affect the binding stability at all.[9] There is no simple explanation for the discrepancy. One suggestion is that FKBP_K35 does not interact with CNA as strongly as the X-ray structure for

TABLE VII. Effects of Mutations on the Stability of the Im9:E9 Complex[a]

Protocol	$\delta\Delta G_{el}$	Energetic decomposition				Interactions[b]	
		$\delta\Delta G_{res}$	$\delta\Delta G_{prot}$	$\delta\Delta G_{int1}$	δG_{int2}	Energy	Distance
			Im9_E30A ($\delta\Delta G_{exp}$ = 1.4; $\delta\Delta$ASA = −104)				
vdW4	2.33	−1.87	−0.74	−0.20	5.14	E9_R54:4.4	OE2-NH1:2.8
SE4	2.90	−6.10	−1.00	0.00	10.00		
SE20	1.39	−1.19	−0.14	−0.14	2.86		
			Im9_E41A ($\delta\Delta G_{exp}$ = 2.1; $\delta\Delta$ASA = −32)				
vdW4	2.13	−0.97	−0.09	−0.64	3.82	E9_K89:1.3	OE1-NZ:4.4
SE4	1.52	−5.00	−0.86	−0.46	7.84	E9_K97:2.5	OE2-NZ:3.2
SE20	1.83	−0.87	−0.10	−0.22	3.02		
			Im9_S50A ($\delta\Delta G_{exp}$ = 2.2; $\delta\Delta$ASA = −5)				
vdW4	0.35	−0.08	−0.09	−0.10	0.62		
SE4	−0.02	−0.58	−0.40	−0.10	1.06		
SE20	0.10	−0.08	−0.04	−0.04	0.26		
			Im9_D51A ($\delta\Delta G_{exp}$ = 5.9; $\delta\Delta$ASA = −26)				
vdW4	1.36	−1.14	−0.07	−0.40	2.88	E9_K89:1.4	OD1-NZ:7.8
SE4	−0.17	−5.12	−0.21	−0.24	5.40		
SE20	0.81	−0.88	−0.01	−0.32	2.02		
			Im9_Y55A ($\delta\Delta G_{exp}$ = 4.6; $\delta\Delta$ASA = −121)				
vdW4	0.53	−0.19	−0.18	0.10	0.80	E9_F86:0.8	OH-O:2.7
SE4	0.32	−0.71	−0.43	0.20	1.26		
SE20	0.18	−0.10	0.00	0.04	0.24		

[a]The list of mutations is from Table 1 of Wallis et al.[13] Calculations were only done for mutations of polar residues that had measured effects of >1 kcal/mol on the binding stability.

TABLE VIII. Effects of Mutations on the Stability of the AChE:Fas Complex[a]

Protocol	$\delta\Delta G_{el}$	Energetic decomposition				Interactions[b]	
		$\delta\Delta G_{res}$	$\delta\Delta G_{prot}$	$\delta\Delta G_{int1}$	δG_{int2}	Energy	Distance
			AChE_D74N ($\delta\Delta G_{exp}$ = 1.9; $\delta\Delta$ASA = 4)				
vdW4	1.16	−0.38	−0.02	−0.58	2.14	Fas_R24: 0.6	OD2-NH2: 8.2
SE4	−0.60	−3.88	0.04	−1.30	4.54	Fas_R37: 0.8	OD1-NH2: 7.4
SE20	0.92	−0.56	0.00	−0.38	1.86		
			AChE_E202Q ($\delta\Delta G_{exp}$ = 0; $\delta\Delta$ASA = 0)				
vdW4	0.46	−0.02	0.00	−0.20	0.68		
SE4	−0.10	−0.42	−0.14	−1.04	1.50		
SE20	0.34	−0.02	−0.04	−0.14	0.54		
			AChE_D280V ($\delta\Delta G_{exp}$ = −0.1; $\delta\Delta$ASA = −1)				
vdW4	0.01	−0.04	−0.07	−0.20	0.32		
SE4	−0.20	−0.05	−0.15	−0.40	0.40		
SE20	0.09	−0.03	0.00	−0.22	0.34		
			AChE_D283N ($\delta\Delta G_{exp}$ = 0.4; $\delta\Delta$ASA = 2)				
vdW4	0.97	−0.66	−0.01	−0.16	1.80	Fas_T8: 0.9	OD1-OG1: 2.5
SE4	0.46	−1.63	0.09	−0.34	2.34	Fas_K25: 0.7	OD2-NZ: 7.3
SE20	0.59	−0.40	−0.01	−0.18	1.18		

[a]The list of AChE single mutations is from Table III of Radic et al.[15]

the complex indicates. In the other seven cases (FKBP_D37V and R42K; Raf1_N64D, K65A, K65E, and K65M; and CD2_K41A), stabilizing effects were predicted but the opposite effects were observed experimentally. As far as the vdW4 calculations are concerned, these discrepancies could be part of the systematic underestimation of destabilization effects. For some of these mutations, there may also be specific reasons. For example, FKBP_D37V and FKBP_R42K involve two residues that form a salt bridge that is important for the stability of FKBP (Batra and Zhou, unpublished), and the mutations may cause compensatory conformational changes that adversely affect the binding with CN. In the modeled structure of the Raf1_N64D mutant, a strong ion pair between Raf1_D64 and Rap1A_R41 was introduced, which might not exist in reality.

Ionic Strength Dependence of Binding Stability

Salt ions in the solvent screen the electrostatic interactions between proteins and thus serve to reduce the association constant. The salt dependence of K_a has been studied on the IL4:IL4BP, Im9:E9, and AChE:Fas complexes.[8,14,15] The calculated ΔG_{el} shows the expected in-

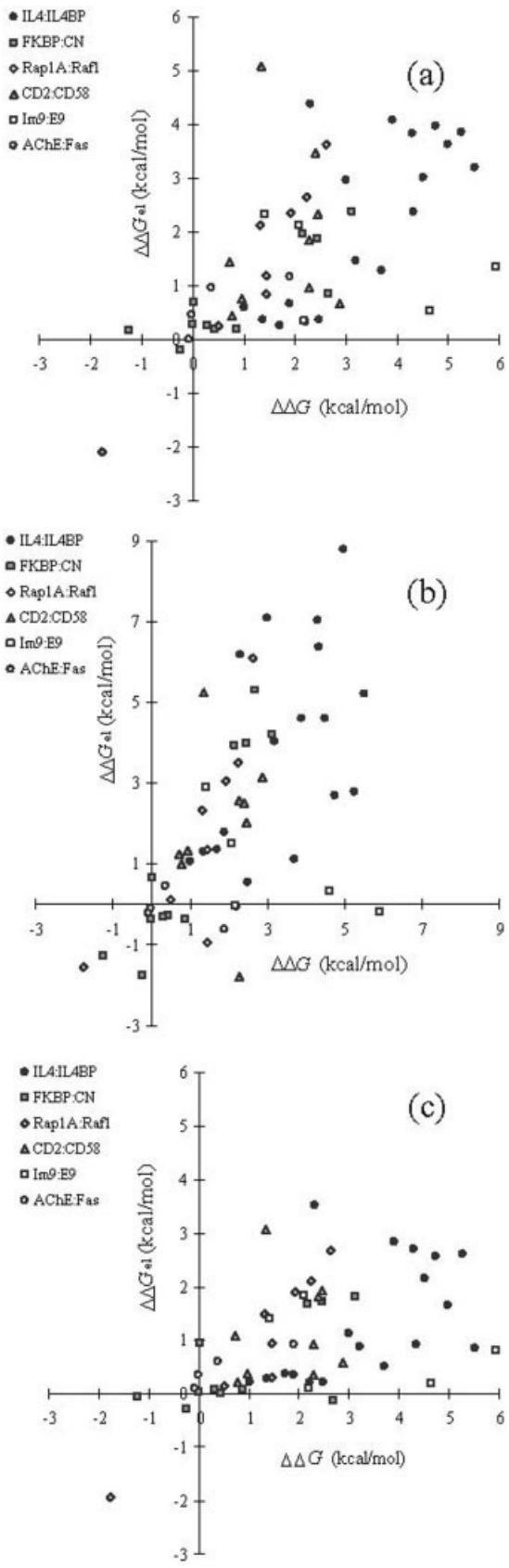

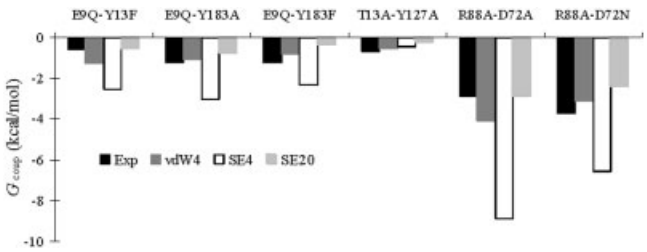

Fig. 5. Comparison of experimental and calculated results for the coupling energies of six pair of residues on the IL4:IL4BP complex. Calculated results from three protocols are shown.

crease with the increase with ionic strength and is in reasonable agreement with experimental data (Fig. 6).

Possible Role of Hydrophobic and van der Waals Interactions

As noted earlier, both the study here on the six protein–protein complexes and the previous study on the barnase-barstar complex found that $\delta\Delta G_{el}$ calculated by vdW4 may account for a major portion of experimental $\delta\Delta G$ but there is room for hydrophobic and van der Waals contributions. When a constant of 0.52 kcal/mol was added to $\delta\Delta G_{el}$ for each of the 55 mutants, the RMSD improved slightly, from 1.46 to 1.37 kcal/mol. In an attempt to account for hydrophobic effects, a term proportional to the buried area of solvent accessibility (ΔASA) upon complex formation was introduced. No improvement could be obtained. However, a modest improvement was obtained when the effect of mutation on the van der Waals interaction energy ΔG_{vdW}, was introduced. After adding $0.44 + 0.073\delta\Delta G_{vdW}$ to $\delta\Delta G_{el}$, the RMSD decreased further to 1.27 kcal/mol.

DISCUSSION

We have carried out extensive calculations on the electrostatic contributions of individual residues to binding stability. For residues making polar or charged interactions across the interface, the experimental mutational effects were found to be largely attributable to electrostatic interactions. Among the three protocols of electrostatic calculations, the one defining the protein van der Waals surface as the dielectric boundary and assigning a protein dielectric constant of 4 showed the best agreement with experimental data. This result reinforces similar findings obtained in previous studies of protein folding stability[3,4] and the barnase-barstar binding stability,[2,36] raises questions about conclusions drawn from using the solvent-exclusion molecular surface as the dielectric boundary.[37,38] The present study also reveals a number of areas for future improvements.

Fig. 4. Comparison of experimental mutational effects on binding stability (horizontal axis) and calculated electrostatic contribution (vertical axis) for a set of 55 mutations over six protein–protein complexes. Calculated results from three protocols are shown: (**a**) vdW4; (**b**) SE4; and (**c**) SE20. The *R* value of correlation between the three sets of calculation results and experimental data is 0.63, 0.59, and 0.52, respectively.

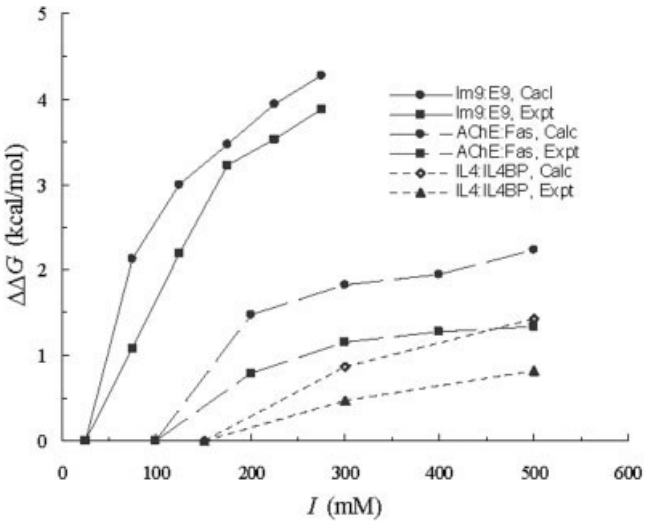

Fig. 6. Experimental and calculated ionic strength dependence of binding energy for the IL4:IL4BP, Im9:E9, and AChE:Fas complexes.

In this study conformational flexibility has been limited to a minimum. (1) For the wild-type protein complex, calculation was restricted to the single conformation determined by X-ray crystallography. Conformational sampling will likely make the calculation results more robust. (2) Each mutation was modeled by energy-minimizing the new side chain in the rigid environment of the rest of the protein. This restriction can be lifted in a number of ways. For example, multiple conformers of the side chain can be introduced, and the neighboring residues can be made flexible when modeling mutation. (3) No conformational changes are allowed upon complex formation. Again, separate conformational sampling by the side chain under mutation and its neighboring residues before and after complex formation can be envisioned.

For the set of mutations selected here for putative dominance of electrostatic contributions to binding stability, van der Waals, and hydrophobic contributions also appeared appreciable. The latter contributions were crudely modeled. More sophisticated parameterization of van der Waals and hydrophobic contributions, coupled with conformational sampling, are expected to improve agreement between calculated and experimental results for mutational effects on binding stability.

The calculated contribution of a single charged residue, like CD2_K51, can be as large as 5 kcal/mol, which translates into a change in K_a of over three orders of magnitudes. This highlights the potential role of electrostatic interactions in modulating binding stability. In addition to CD2_K51, six other residues were calculated to contribute more than 3 kcal/mol to binding stability through electrostatic interactions. These are IL4_R88, D67, and D72, FKBP_K35, Raf1_R89, CD2_R48. Each of these residues generally forms a cluster of interactions, with a strong salt bridge surrounded by several other polar interactions. This interaction pattern may be introduced to protein–protein interfaces for enhanced binding stability. It is known that thermophilic oligomeric proteins typically have enriched ion pair clusters in the interfaces between subunits. The interaction pattern may also serve as a target for antagonists. Potentially an antagonist that disrupts the clustered interactions may lower the protein–protein association constant by orders of magnitudes.

Electrostatic interactions may also be very important for cross-species specificity. For example, E9 DNase shows high selectivity for Im9 over other immunity proteins. Charged residues can contribute to such selectivity by either positive design, e.g., through a clustered interaction pattern noted above, or negative design, e.g., through the burial of charged residues. Calculation methods presented here and future refinements will shed new light on how electrostatic interactions can be used to control cross-species specificity.

In summary, we have tackled the difficult problem of predicting the effects of point mutations on protein binding stability by focusing on a set of mutations with putative dominance of electrostatic contribution. The calculated electrostatic contributions showed some agreement with experiment and will serve as a guide for future refinement in electrostatic calculation and inclusion of van der Waals and hydrophobic effects.

ACKNOWLEDGMENTS

This work was supported in part by NIH grant GM58187. We thank Harianto Tjong for carrying out calculations of van der Waals interaction energy on the protein complexes.

REFERENCES

1. Brooijmans N, Sharp KA, Kuntz ID. Stability of macromolecular complexes. Proteins 2002;48:645–653.
2. Dong F, Vijayakumar M, Zhou H-X. Comparison of calculation and experiment implicates significant electrostatic contributions to the binding stability of barnase and barstar. Biophys J 2003;85:49–60.
3. Vijayakumar M, Zhou H-X. Salt bridges stabilize the folded structure of barnase. J Phys Chem B 2001;105:7334–7340.
4. Dong F, Zhou H-X. Electrostatic contributions to T4 lysozyme stability: solvent-exposed charges versus semi-buried salt bridges. Biophys. J. 2002;83: 1341–1347.
5. Zhou H-X. Toward the physical basis of thermophilic proteins: linking of enriched polar interactions and reduced heat capacity of unfolding. Biophys J 2002;83:3126–3133.
6. Zhou H-X, Dong F. Electrostatic contributions to the stability of a thermophilic cold shock protein. Biophys J 2003;84:2216–2222.
7. Zhang J-L, Simeonowa I, Wang Y, Sebald W. The high-affinity interaction of human IL-4 and the receptor α chain is constituted by two independent binding clusters. J Mol Biol 2002;315:399–407.
8. Shen B-J, Hage T, Sebald W. Global and local determinants for the kinetics of interleukin-4/interleukin-4 receptor α chain interaction. A biosensor study employing recombinant interleukin-4-binding protein. Eur J Biochem 1996;240:252–261.
9. Yang D, Rosen MK, Schreiber SL. A composite FKBP12-FK506 surface that contacts calcineurin. J Am Chem Soc 1993;115:819–820.
10. Futer O, Decenzo MT, Aldape RA, Livingston DJ. FK506 binding protein mutational analysis. J Biol Chem 1995;270:18935–19840.
11. Nassar N, Horn G, Herrmann C, Block C, Janknecht R, Wittinghofer A. Ras/Rap effector specificity determined by charge reversal. Nat Struct Biol 1996;3:723–729.
12. Kim M, Sun Z-YJ, Byron O, Campbell G, Wagner G, Wang J-h, Reinherz EL. Molecular dissection of the CD2-CD58 counter-receptor interface identifies CD2 Tyr86 and CD58 Lys residues as the functional "hot spot." J Mol Biol 2001;312:711–720.

13. Wallis R, Leung K-Y, Osborne MJ, James R, Moore GR, Kleanthous C. Specificity in protein-protein recognition: conserved Im9 residues are the major determinations of stability in the colicin E9 Dnase-Im9 complex. Biochemistry 1998;37:476–485.
14. Wallis R, Moore GKJames R, Kleanthous C. Protein-protein interactions in colicin E9 DNase-immunity protein complexes. 1. Diffusion-controlled association and femtomolar binding for the cognate complex. Biochemistry 1995;34:13743–13750.
15. Radic Z, Kirchhoff PD, Quinn DM, McCammon JA, Taylor P. Electrostatic influence on the kinetics of ligand binding to acetylcholinesterase. J Biol Chem 1997;272:23265–23277.
16. Hage T, Sebald W, Reinemer P. Crystal structure of the interleukin-4/receptor alpha chain complex reveals a mosaic binding interface. Cell 1999;97:271–281.
17. Zhou H-X. Disparate ionic-strength dependence of on and off rates in protein–protein association. Biopolymers 2001;59:427–433.
18. Griffith JP, Kim JL, Kim EE, Sintchak MD, Thomson JA, Fitzgibbon MJ, Fleming MA, Caron PR, Hsiao K, Navia MA. X-ray structure of calcineurin inhibited by the immunophilin-immunosuppressant FKBP12-FK506 complex. Cell 1995;82:507–522.
19. Nassar N, Horn C, Herrmann C, Scherer A, McCormick F, Wittinghofer A. The 2.2 Å crystal structure of the Ras-binding domain of the serine/threonine kinase c-Raf1 in complex with Rap1A and a GTP analogue. Nature 1995;375:554–560.
20. Wang J-h, Smolyar A, Tan K, Liu J-h, Kim M, Sun Z-y J, et al. Structure of a heterophilic adhesion complex between the human CD2 and CD58 (LFA-3) counterreceptors. Cell 1999;97:791–803.
21. Kuhlmann UC, Pommer AJ, Moore GR, James R, Kleanthous C. Specificity in protein-protein interactions: the structural basis for dual recognition in endonuclease colicin-immunity protein complexes. J Mol Biol 2000;301:1163–1178.
22. Bourne Y, Taylor P, Marchot P. Acetylcholinesterase inhibition by fasciculin: crystal structure of the complex. Cell 1995;83:503–512.
23. Sharp KA, Honig B. Electrostatic interactions in macromolecules: theory and applications. Annu Rev Biophys Biophys Chem 1990; 19:301–332.
24. Madura JD, Briggs JM, Wade RC, Davis ME, Luty BA, Ilin A, Antosiewicz J, Gilson MK, Bagheri B, Scott LR, McCammon JA. Electrostatics and diffusion of molecules in solution: simulations with the University of Houston Brownian Dynamics program. Comput Phys Comm 1995;91:57–95.
25. Kuhn B, Kollman PA. Binding of a diverse set of ligands to avidin and streptavidin: an accurate quantitative prediction of their relative affinities by a combination of molecular mechanics and continuum solvent models. J Med Chem 2000;43:3786–3791.
26. Gohlke H, Case DA. Converging free energy estimates: MM-PB(GB)SA studies on the protein-protein complex Ras-Raf. J Comput Chem 2004;25:238–250.
27. Swanson JM, Henchman RH, McCammon JA. Revisiting free energy calculations: a theoretical connection to MM/PBSA and direct calculation of the association free energy. Biophys J 2004;86: 67–74.
28. Yu Z, Jacobson MP, Friesner RA. What role do surfaces play in GB models? A new-generation of surface-generalized born model based on a novel Gaussian surface for biomolecules. J Comput Chem 2005;27:72–89.
29. Swanson JMJ, Mongan J, McCammon JA. Limitations of atom-centered dielectric functions in implicit solvent models. J Phys Chem B 2005;109:14769–14772.
30. Schreiber G, Fersht AR. Energetics of protein-protein interactions: analysis of the barnase-barstar interface by single mutations and double mutant cycles. J Mol Biol 1995;248:478–486.
31. Antosiewicz J, McCammon JA, Gilson MK. Prediction of pH-dependent properties of proteins. J Mol Biol 1994;238:415–436.
32. Case DA, Pearlman DA, Caldwell JW, Cheatham III TE, Wang J, Ross WS, Simmerling CL, et al. Amber Version 7.0, University of California: San Francisco, CA. 2002.
33. Jorgensen WL, Maxwell DS, Tirado-Rives J. Development and testing of the OPLS all-atom force field on conformational energetics and properties of organic liquids. J Am Chem Soc 1996;118: 11225–11236.
34. Bondi A. van der Waals volumes and radii. J Phys Chem 1964;68: 441–451.
35. Kabsch W, Sander C. Dictionary of protein secondary structures: pattern recognition of hydrogen bonded and geometrical features. Biopolymers 1983;22: 2577–2637.
36. Wang T, Tomic S, Gabdoulline RR, Wade RC. How optimal are the binding energetics of barnase and barstar? Biophys J 2004;87: 1618–1630.
37. Lee L-P, Tidor B. Optimization of binding electrostatics: charge complementarity in the barnase-barstar protein complex. Protein Sci 2001;10:362–377.
38. Sheinerman FB, Honig B. On the role of electrostatic interactions in the design of protein-protein interfaces. J Mol Biol 2002;318:161–177.